

# In-beam $\gamma$ -ray spectroscopy toward the proton dripline: The curious case of $^{32}\text{Ar}$

T. Beck<sup>1,\*</sup>, A. Gade<sup>1,2</sup>, B. A. Brown<sup>1,2</sup>, Y. Utsuno<sup>3,4</sup>, D. Weisshaar<sup>1,5</sup>, D. Bazin<sup>1,2</sup>, K. W. Brown<sup>1,5</sup>, R. J. Charity<sup>6</sup>, P. J. Farris<sup>1,2</sup>, S. A. Gillespie<sup>1</sup>, A. M. Hill<sup>1,2</sup>, J. Li<sup>1</sup>, B. Longfellow<sup>1,2,†</sup>, W. Reviol<sup>7</sup>, and D. Rhodes<sup>1,2,‡</sup>

<sup>1</sup>Facility for Rare Isotope Beams, Michigan State University, East Lansing, Michigan 48824, USA

<sup>2</sup>Department of Physics and Astronomy, Michigan State University, East Lansing, Michigan 48824, USA

<sup>3</sup>Advanced Science Research Center, Japan Atomic Energy Agency, Tokai, Ibaraki 319-1195, Japan

<sup>4</sup>Center for Nuclear Study, University of Tokyo, Hongo, Bunkyo-ku, Tokyo 113-0033, Japan

<sup>5</sup>Department of Chemistry, Michigan State University, East Lansing, Michigan 48824, USA

<sup>6</sup>Department of Chemistry, Washington University, St. Louis, Missouri 63130, USA

<sup>7</sup>Physics Division, Argonne National Laboratory, Argonne, Illinois 60439, USA



(Received 6 December 2024; accepted 12 March 2025; published 7 April 2025)

High-resolution in-beam  $\gamma$ -ray spectroscopy was used to study excited states of the neutron-deficient nucleus  $^{32}\text{Ar}$  populated in fast-beam induced four- and six-nucleon removal reactions from  $^{36,38}\text{Ca}$ . One new  $\gamma$ -ray transition and indications for an additional two were found, allowing for a glimpse at the level scheme beyond the  $2_1^+$  state. The nature of the new 1900(4)-keV transition is discussed in the context of the known energy spectrum of the mirror nucleus  $^{32}\text{Si}$  and shell-model calculations using the FSU and SDPF-M cross-shell effective interactions. Its resulting parent state at 3767(5) keV, more than 1.3 MeV above the proton separation energy, is tentatively assigned to have mixed  $sd$ -shell and 2p-2h character. It might either be the mirror of the  $J^\pi = 2_2^+$  state of  $^{32}\text{Si}$  at 4230.8(8) keV, but with a decay branch favoring a transition to the  $2_1^+$  over the ground state, or the mirror of the 4983.9(11)-keV state with quantum numbers  $0^+$ . The resulting mirror-energy differences of  $-473(5)$  and  $-1218(5)$  keV are both sizable when compared to systematics; in the latter case the result would, in fact, be among the largest reported to date in the nuclear chart or suggest the potential existence of an additional, hitherto unidentified, low-lying  $0^+$  state of  $^{32}\text{Si}$ .

DOI: [10.1103/PhysRevC.111.044306](https://doi.org/10.1103/PhysRevC.111.044306)

## I. INTRODUCTION

Neutron-deficient nuclei, i.e., nuclei lighter than the corresponding  $\beta$ -stable isotopes with, in some cases larger number of protons  $Z$  than neutrons  $N$ , are key for understanding nucleosynthesis mechanisms such as the  $rp$  process [1], might exhibit modes of proton radioactivity [2], and can provide a complementary view on nuclear forces [3]. Regarding the proton dripline, the progress at rare-isotope facilities [4] has established its location up to medium-mass nuclei [5] and nuclear theory has yielded *ab initio* predictions of it up to iron [6]. In the  $sd$  shell, spanning from  $^{16}\text{O}$  ( $Z, N = 8$ ) to  $^{40}\text{Ca}$  ( $Z, N = 20$ ), spectroscopic information on excited states of many neutron-deficient isotopes up to or even beyond the dripline is available. Recent experimental highlights from this region include the observation and first spectroscopy of the three-proton emitter  $^{31}\text{K}$ , located four neutrons beyond the dripline [7], or the spectroscopy of  $^{35}\text{Ca}$  potentially suggesting doubly-magic character of  $^{36}\text{Ca}$  [8].

The present work is focused on the neutron-deficient  $^{32}\text{Ar}$  ( $Z = 18, N = 14$ ) nucleus. It is the lightest proton-bound, even-even argon isotope, as two-proton decay was observed for the ground-state of  $^{30}\text{Ar}$  [9]. The low-lying structure of its astrophysically interesting, heavier isotopic neighbors  $^{33,34}\text{Ar}$  is known from combined particle- $\gamma$  spectroscopy [10–12]. Previous studies involving  $^{32}\text{Ar}$  mainly concerned its mass [13] and  $\beta$ -decay properties [14, and references therein] for the search of physics beyond the standard model. Removal of a strongly-bound neutron from  $^{32}\text{Ar}$  [15] triggered the discovery of the strong correlation between the experimental-to-theoretical cross-section ratio,  $R_s$ , and the asymmetry of proton and neutron binding in heavy-ion-induced nucleon-removal reactions [16–18]. Information on its excited states, on the other hand, remained sparse. Hitherto, only the  $2_1^+$  state of  $^{32}\text{Ar}$  at 1867(8) keV [19] was identified experimentally using scintillator arrays [20,21] and segmented germanium detectors [22]. Excited states above the comparatively low proton separation energy of  $S_p(^{32}\text{Ar}) = 2455(4)$  keV [23], revealing the proximity of  $^{32}\text{Ar}$  to the proton continuum, remained unknown. The present work provides new information on excitations beyond the  $2_1^+$  state, populated in the  $^{197}\text{Au}(^{36}\text{Ca}, ^{32}\text{Ar} + \gamma)X$  and  $^9\text{Be}(^{38}\text{Ca}, ^{32}\text{Ar} + \gamma)X$  multinucleon removal reactions, from first high-resolution in-beam  $\gamma$ -ray spectroscopy using a modern tracking array.

\*Contact author: beck@frib.msu.edu

†Present address: LPC Caen, 14050 Caen Cedex, France.

‡Present address: Lawrence Livermore National Laboratory, Livermore, California 94550, USA.

## II. EXPERIMENT AND RESULTS

The reaction channels discussed here share the same secondary beams of unstable  $^{36,38}\text{Ca}$  nuclei as the experiments reported in Refs. [24] and [25–29], respectively. They were produced through fragmentation of a stable  $^{40}\text{Ca}$  beam, accelerated to 140 MeV/u by the Coupled Cyclotron Facility of the National Superconducting Cyclotron Laboratory [30], on a 799-mg/cm<sup>2</sup>  $^9\text{Be}$  production target. The fragments were subsequently separated in the A1900 fragment separator [31], using a 300-mg/cm<sup>2</sup> aluminum wedge degrader and with the momentum acceptance restricted to  $\Delta p/p = 0.25\%$ . The resulting beams, which for  $^{36}\text{Ca}$  and  $^{38}\text{Ca}$  had purities of 11% [24] and 85%, were impinged on 257- and 188-mg/cm<sup>2</sup>-thick  $^{197}\text{Au}$  and  $^9\text{Be}$  secondary reaction targets, respectively, located at the target position of the S800 magnetic spectrograph [32]. Incoming species were identified from their time-of-flight differences taken between two plastic scintillators at the exit of the A1900 and the object position of the S800 analysis beam line. Outgoing projectile-like reaction products were selected on an event-by-event basis in the S800 focal plane [33] using time-of-flight differences taken between two plastic scintillators at the object position of the analysis beam line and the S800 focal plane, and their energy loss was measured in the spectrograph's ionization chamber.

Prompt  $\gamma$  rays emitted in flight by the excited reaction products were detected with the high-resolution tracking array GRETINA [34,35], comprising twelve detector modules of four 36-fold segmented germanium crystals each. Employing online signal decomposition, the spatial coordinates of the  $\gamma$ -ray interaction points with the highest energy deposition in GRETINA are identified and used for event-by-event Doppler correction, furthermore incorporating information on the momentum vector of  $^{32}\text{Ar}$  in the exit channel, exploiting the track-reconstruction capabilities of the S800 spectrograph. Resulting  $\gamma$ -ray spectra of  $^{32}\text{Ar}$  from both production pathways are displayed in Fig. 1. The spectrum [Fig. 1(b)] produced in the  $^9\text{Be}(^{38}\text{Ca}, ^{32}\text{Ar} + \gamma)X$  reaction features peaks at 1866(3) and 1900(4) keV. The former is attributed to the ground-state transition of the  $2_1^+$  state at 1867(8) keV [19] and corroborates the results of Refs. [21,22], which report a higher excitation energy than Cottle *et al.* [20]. The  $\gamma$ -ray transition at 1900(4) keV was unknown until now. Both peaks can also be identified in the  $\gamma$ -ray spectra [Fig. 1(a)] following the  $^{197}\text{Au}(^{36}\text{Ca}, ^{32}\text{Ar} + \gamma)X$  reaction, though with lower statistics. The different intensity ratios  $I_\gamma(1900)/I_\gamma(1866) = 54^{+46}_{-29}\%$  and 17(7)% obtained in the  $^{36}\text{Ca}$ - and  $^{38}\text{Ca}$ -induced reactions, respectively, might be traced to differing population characteristics of the four- and six-nucleon removal reactions [36,37]. Also, the  $\gamma$ -ray spectrum of  $^{32}\text{Ar}$  produced in the  $^9\text{Be}(^{37}\text{Ca}, ^{32}\text{Ar} + \gamma)X$  reaction, which is shown in Ref. [21], suggests the existence of a second peak at around 1.9 MeV, although it is not explicitly discussed in that publication.

Limited statistics do not allow for the use of  $\gamma\gamma$  coincidences to clarify the relation between both  $\gamma$  rays. Figure 2(b) shows the total projection of the  $\gamma\gamma$  coincidence matrix with the two peaks identified in the  $\gamma$ -ray singles spectrum clearly visible. The spectrum in coincidence with the most prominent  $2_1^+ \rightarrow 0_1^+$  transition has at most one count in any bin above

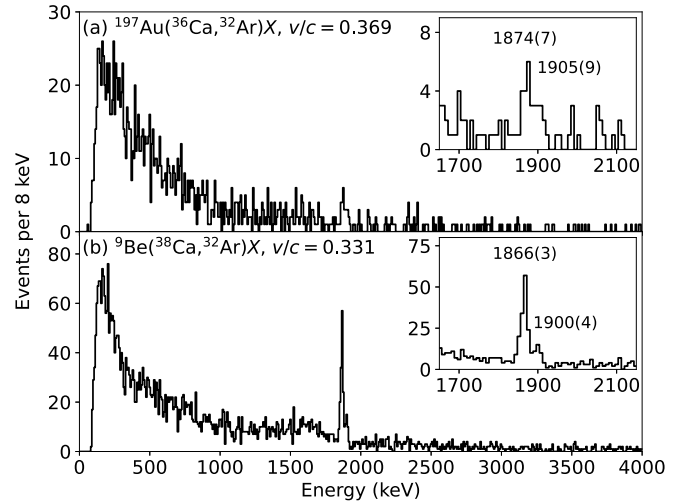


FIG. 1. Doppler-reconstructed  $\gamma$ -ray spectra of  $^{32}\text{Ar}$  produced in the (a)  $^{197}\text{Au}(^{36}\text{Ca}, ^{32}\text{Ar} + \gamma)X$  and (b)  $^9\text{Be}(^{38}\text{Ca}, ^{32}\text{Ar} + \gamma)X$  reactions. The insets show the region around the  $2_1^+ \rightarrow 0_1^+$  transition, unveiling the existence of a new  $\gamma$ -ray transition at 1900(4) keV. The difference in resolution between both reactions can be explained by the strongly differing stopping in the gold and beryllium targets.

1 MeV. However, the projected coincidence matrix might reveal the existence of two additional, previously unknown  $\gamma$ -ray transitions. They are also identified at 2134(6) and 3161(7) keV in Fig. 2(a), which shows the  $\gamma$ -ray singles spectra with nearest-neighbor add-back [35] included.

Since it is not possible to determine whether the 1866(3) and 1900(4)-keV  $\gamma$  rays form a cascade, two possible placements for the latter need to be considered. The new  $\gamma$  ray corresponds to either the ground-state transition of an excited

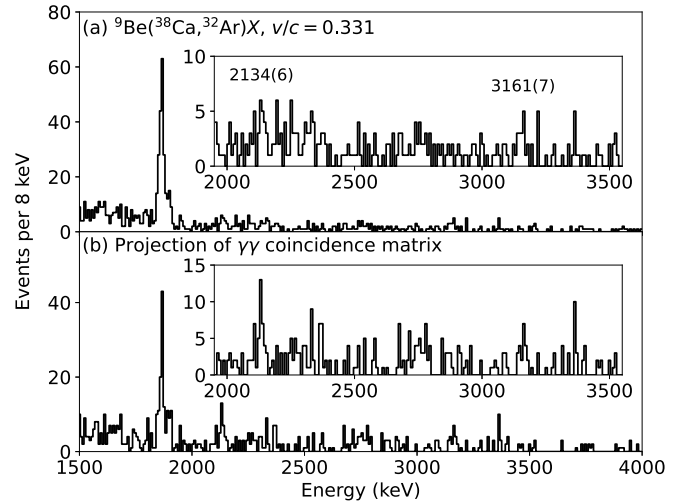


FIG. 2. (a) Doppler-reconstructed  $\gamma$ -ray spectrum of  $^{32}\text{Ar}$  produced in the  $^9\text{Be}(^{38}\text{Ca}, ^{32}\text{Ar} + \gamma)X$  reaction and using nearest-neighbor add-back [35]. (b) Projection of the  $\gamma\gamma$  coincidence matrix from the same reaction and using the same low-energy cutoff as the  $\gamma$ -ray singles spectra shown in Figs. 1 and 2(a). The insets enlarge the high-energy part of the spectrum at the same energy dispersion and suggest the existence of two candidate  $\gamma$ -ray transitions of  $^{32}\text{Ar}$ .

state of  $^{32}\text{Ar}$  at 1900(4) keV or the decay of a proton-unbound state at 3767(5) keV into the  $2_1^+$  level. Guidance can be obtained from the level scheme of the mirror nucleus  $^{32}\text{Si}$  [19]. Its  $2_1^+$  state is found at 1941.4(3) keV [19]; this corresponds to a conventional mirror-energy difference (MED) of  $-75(3)$  keV for the  $^{32}\text{Ar} / ^{32}\text{Si}$  pair. There is no state in close proximity to it; the  $2_2^+$  state is found more than 2 MeV higher in energy. Based on this observation, the existence of a 1900(4)-keV state of  $^{32}\text{Ar}$  can be refuted since it would correspond to an MED of more than 2.3 MeV. This is well beyond the range normally attributed to Coulomb-interaction induced isospin breaking [38] and even exceeds the “colossal” MED of the  $0_2^+$  state in the  $^{36}\text{Ca} / ^{36}\text{S}$  mirror pair [39] by a factor of 4. It can, instead, be concluded that the 1900(4)-keV transition most likely stems from the  $\gamma$  decay of a proton-unbound state at 3767(5) keV into the  $2_1^+$  level.

### III. DISCUSSION

In order to clarify the nature of the new 3767(5)-keV state of  $^{32}\text{Ar}$ , further input from theory is needed. Since the lowest-lying known negative-parity states of  $^{32}\text{Si}$  are found at around 5 MeV, the level structure is first compared to shell-model calculations carried out with the code NuShellX [40] and using the Florida State University (FSU) cross-shell effective interaction [41,42] in the extensive *spsdfp* model space. The level scheme calculated for  $A = 32$  is in good agreement with the available experimental data for  $^{32}\text{Si}$ . The structure of the calculated states can be characterized by  $\Delta$ , which signifies the number of nucleons promoted from the  $sd$  to the  $pf$  shell. In this notation, states with  $\Delta = 0$  are of  $sd$ -shell origin and those with  $\Delta = 1$  have negative parity and cross-shell nature. The  $0_1^+$  and  $2_{1,2}^+$  states for  $A = 32$ , for instance, are of  $sd$ -shell origin. The  $3_1^-$  and  $5_1^-$  states found at 5288.8(8) and 5581(4) keV [19] in  $^{32}\text{Si}$ , are predicted at 5897 and 6003 keV, respectively. Above  $S_p(^{32}\text{Ar}) = 2455(4)$  keV [23], all states with  $\Delta = 0$  and 1 calculated in the shell model are predicted to exclusively proton decay to final states of  $^{31}\text{Cl}$ . Thus, the conjectured state at 3767(5) keV must be attributed to a  $\Delta = 2$  configuration in the FSU spectrum. Since  $\gamma$ -ray transitions are possible only between states differing by at most one unit in  $\Delta$ , the wave function must also feature components with  $\Delta = 0$ . The delicate interplay of these two configurations can produce an excited state which has at least comparable proton- and  $\gamma$ -decay probabilities, with the latter reaching the  $sd$ -shell  $2_1^+$  state. Due to the low  $Q$  value,  $S_{2p}(^{32}\text{Ar}) = 2719.0(18)$  keV [23], the probability for  $2p$  decay of this state is likely negligible [43]. Since the FSU cross-shell effective interaction deals in pure  $\Delta$  configurations, it does not yield information on an admixed state. Its properties can instead be studied using the SDPF-M cross-shell effective interaction [44,45] which allows for the mixing of different particle-hole configurations between the  $sd$  and  $pf$  shells. With the model space truncated to excitations with at most  $\Delta = 4$ , the calculations, which were performed with the code KSHELL [46], yield dominant  $sd$ -shell nature for the  $0_1^+$  and  $2_{1,2}^+$  states in agreement with the FSU results. An intruder  $0_2^+$  state, characterized by an 84% 2p-2h component in its wave function, is predicted at

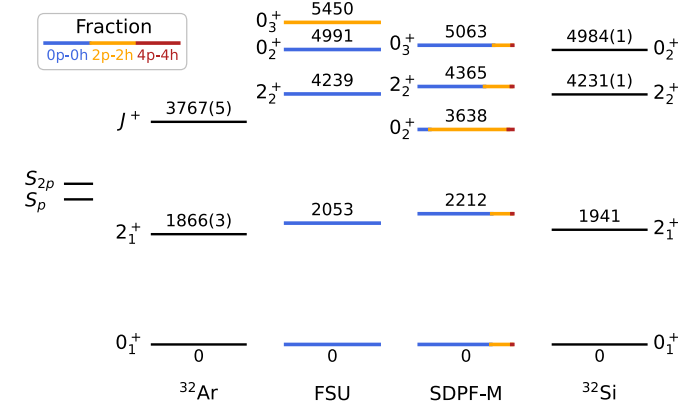


FIG. 3. Comparison of excitation energies in keV obtained from shell-model calculations with the FSU and SDPF-M cross-shell excitations to the mirror nuclei  $^{32}\text{Ar}$  and  $^{32}\text{Si}$ . The lines marking levels obtained from the shell model are color-coded by the fractions of 0p-0h (blue), 2p-2h (orange), and 4p-4h (red) configurations in their wave functions. Energies and quantum numbers of excited states of  $^{32}\text{Si}$  and proton-separation energies of  $^{32}\text{Ar}$  are taken from Refs. [19] and [23], respectively.

3638 keV and is absent from the FSU spectrum in this energy region. The next higher  $0_2^+$  state (80% 0p-0h) is found at 5063 keV, very close to the  $\Delta = 0$   $0_2^+$  state placed at 4991 keV in the calculations using the FSU effective interaction. A comparison of the energy levels predicted by the FSU and SDPF-M calculations is shown in Fig. 3.

Experimental information on 2p-2h states is available in the vicinity of the  $^{32}\text{Ar} / ^{32}\text{Si}$  mirror pair. In  $^{34}\text{Si}$ , the  $\Delta = 2$   $0^+$  state is found at 2719(3) keV [47], in agreement with shell-model calculations using the FSU effective interaction [48]. In neighboring  $^{32}\text{Si}$ , a  $0^+$  state is found at 4983.9(11) keV [19], which decays via  $\gamma$ -ray emission to the  $2_1^+$  state with a half-life of  $T_{1/2} < 0.3$  ps [49]. Its population in the  $^{30}\text{Si}(t, p)$  reaction is reported to be too strong for a pure  $sd$ -shell nature, and distorted-wave Born approximation (DWBA) calculations using  $sd$ -shell transfer amplitudes [50] fail to adequately describe its angular distribution [51]. Fortune *et al.* noted that a small  $(sd)^{-2}(f_{7/2})^2$  admixture of less than 20% to the state’s wave function suffices to reproduce the measured cross section [51]. This finding, along with the state’s excitation energy, fits exceptionally well to the  $0_3^+$  state from the SDPF-M spectrum, which contains a 20% 2p-2h contribution to its wave function.

As is evident from Fig. 3, two potential assignments for the new 3767(5)-keV state of  $^{32}\text{Ar}$  must be considered. It may be identified as the intruder  $0_2^+$  state predicted in the shell-model calculations using the SDPF-M effective interaction, which yields a close reproduction of the excitation energy. However, this state is predicted to predominantly proton decay to the  $3/2^+$  and  $(1/2^+)$  states of  $^{31}\text{Cl}$  with  $Q$  values of 1.312 and 0.575 MeV, respectively, as is evident from Table I, which collects single-particle proton-decay half-lives  $T_{1/2}^{sp}(p)$  and spectroscopic factors  $C^2S$  obtained from the FSU and SDPF-M shell-model effective interactions. With  $T_{1/2}(p) = T_{1/2}^{sp}(p)/C^2S$ , the spectroscopic factors must be less

TABLE I. Compilation of single-particle proton-decay half-lives  $T_{1/2}^{sp}(p)$  and spectroscopic factors  $C^2S$  from the FSU and SDPF-M shell-model effective interactions. Comparison to  $\gamma$ -decay half-lives  $T_{1/2}$  measured for  $^{32}\text{Si}$  [19] reveals the predominance of the proton-decay channel to final states of  $^{31}\text{Cl}$  for proton-unbound states of  $^{32}\text{Ar}$  with  $\Delta = 0$  or 1.

Single-particle proton decay			$C^2S$		$^{32}\text{Si}$ [19]	
$J_f^\pi$	$(n, l, j)$	$T_{1/2}^{sp}(p)$ (ps)	FSU	SDPF-M	$J_i^\pi$	$T_{1/2}$ (ps)
$3/2^+$	$1d_{3/2}$		1.98	1.50	$0_1^+$	
$3/2^+$	$2s_{1/2}$		0.011	0.0011	$2_1^+$	0.78(22)
$3/2^+$	$1d_{3/2}$	$1.4 \times 10^{-6}$	0.0076	0.18 <sup>a</sup>	$0_2^+$	$<0.30$
$3/2^+$	$1d_{3/2}$	$1.4 \times 10^{-6}$	0 <sup>b</sup>	0.010	$0_3^+$	
$3/2^+$	$2s_{1/2}$	$3.0 \times 10^{-8}$	0.082	0.021	$2_2^+$	0.26(9)
$3/2^+$	$2p_{3/2}$	$7.2 \times 10^{-8}$	0.050		$3_1^-$	0.15(35)
$3/2^+$	$1f_{7/2}$	$1.7 \times 10^{-5}$	0.77		$5_1^-$	$27(2) \times 10^3$
$1/2^+$	$2s_{1/2}$		1.26	1.18	$0_1^+$	
$1/2^+$	$2s_{1/2}$	$3.1 \times 10^{-5}$	0.31	0.0021 <sup>a</sup>	$0_2^+$	$<0.30$
$1/2^+$	$2s_{1/2}$	$3.1 \times 10^{-5}$	0 <sup>b</sup>	0.11	$0_3^+$	

<sup>a</sup>This state has 84%  $\Delta = 2$ .

<sup>b</sup>This state has  $\Delta = 2$ .

than about  $10^{-6}$  to allow for  $\gamma$  and proton decays to compete. The calculated values for the states discussed here, however, are much larger. The small spectroscopic factor of 0.0076 for the proton decay of the  $0_2^+$  state to the  $3/2^+$  ground state of  $^{31}\text{Cl}$  could be made arbitrarily close to zero by a small mixing with the  $0_1^+$  state. But this mixing will not significantly change the larger spectroscopic factor of  $C^2S = 0.31$  for its decay to the first-excited ( $1/2^+$ ) state of  $^{31}\text{Cl}$ , maintaining the predominance of proton decay over  $\gamma$  decay. A comparison to the level scheme of  $^{32}\text{Si}$  would make the 3767(5)-keV state of  $^{32}\text{Ar}$  the mirror of the 4983.9(11)-keV  $0^+$  state of  $^{32}\text{Si}$  [19], resulting in a mirror-energy difference of  $-1218(5)$  keV. This would be among the largest MEDs ever suggested, surpassing even the  $0_2^+$  state of the  $^{36}\text{Ca} / ^{36}\text{S}$  mirror pair [39] and large continuum-driven energy differences for the  $A = 13$  and 16 pairs  $^{13}\text{N} / ^{13}\text{C}$  [52,53] and  $^{16}\text{F} / ^{16}\text{N}$  [54], respectively, and rivaling the MEDs put forth for  $^{24}\text{Si} / ^{24}\text{Ne}$  [55] and  $^{14}\text{O} / ^{14}\text{C}$  [56]. However, the dominant *sd*-shell character of the known  $0_2^+$  state of  $^{32}\text{Si}$  [51] might suggest the existence of an additional, until now unidentified, lower-lying  $0^+$  state of  $^{32}\text{Si}$ . In the  $^{30}\text{Si}(t, p)$  experiments of Fortune *et al.* [51], its signal might have been obscured by reactions on target contaminants in the energy region expected for a normal-sized MED without weak-binding effects [38]. In the vicinity of the  $^{32}\text{Ar} / ^{32}\text{Si}$  mirror pair,  $0_2^+$  states are indeed found in this energy region; at 3667.4(8) keV [57] for the  $N = 14$  isotope  $^{30}\text{S}$ , 3873(3) keV [58] for  $^{34}\text{Ar}$ , and at 3787.72(5) keV [57] for  $^{30}\text{Si}$ .

Assuming instead that the 3767(5)-keV state is the mirror of the  $2_2^+$  state of  $^{32}\text{Si}$  at 4230.8(8) keV [19] yields an MED of  $-473(5)$  keV, which is still large when compared to systematics [38] but significantly smaller than for the  $0^+$  assignment discussed above. In  $^{32}\text{Si}$ , the  $2_2^+$  state decays predominantly to the ground state in contrast to the shell-model calculations with the FSU and SDPF-M effective interactions, which predict strong transitions to the  $2_1^+$

and  $0_2^+$  states, respectively. Using the known branching ratio  $I_\gamma(2_2^+ \rightarrow 2_1^+)/I_\gamma(2_2^+ \rightarrow 0_1^+) = 0.61(5)$  [19], a peak containing 22(8) counts against an average background of one count per bin should be clearly identifiable at 3767(5) keV in the spectrum of Fig. 1(b). Small admixtures from energetically close-lying states to the  $2_2^+$  state might, similarly to the situation encountered for some rare-earth nuclei [59,60], have altered its decay characteristics to feature a dominant transition to the ground state of  $^{32}\text{Si}$ .

Lastly, it has to be examined if a state with partial 2p-2h nature can be populated in the  $^{197}\text{Au}(^{36}\text{Ca}, ^{32}\text{Ar})X$  and  $^9\text{Be}(^{38}\text{Ca}, ^{32}\text{Ar})X$  reactions discussed here. The weakening of the  $Z = 20$  shell gap in the region of the neutron-deficient calcium isotopes, which was recently further corroborated through invariant-mass spectroscopy of  $^{34}\text{K}$  and  $^{37,38}\text{Sc}$  [61], leads to an increased proton *pf*-shell occupancy in the ground states of  $^{36,38}\text{Ca}$  [24,28]. Using the ZBM2 shell-model effective interaction [62] in the  $(1d_{3/2}, 2s_{1/2}, 1f_{7/2}, 2p_{3/2})$  model space, fractions of 31%, 28%, and 25% are found for the 2p-2h proton intruder components in the ground-state wave functions of  $^{36,37,38}\text{Ca}$ , respectively. Hence, few-nucleon removal reactions from these configurations, as employed here, may indeed populate final states of  $^{32}\text{Ar}$  with two protons in the *pf* shell. This might furthermore explain why the 3767(5)-keV state appears to have also been populated in the  $^9\text{Be}(^{37}\text{Ca}, ^{32}\text{Ar})X$  reaction [21]. For two-neutron removal from  $^{34}\text{Ar}$ , on the other hand, population cross sections can be obtained from a combination of eikonal reaction dynamics and SDPF-M two-nucleon amplitudes [63,64]. These calculations predict a vanishing population probability for the intruder  $0_2^+$  state and comparable cross sections for the  $2_1^+$  and  $2_2^+$  states. In the experiment of Yoneda *et al.* only the ground-state decay of the  $2_1^+$  state has been observed [22], whereas a proton decay of the  $2_2^+$  state, as expected from the half-lives given in Table I, would have remained undetected.

#### IV. SUMMARY

In summary, excited states of the neutron-deficient, near-dripline nucleus  $^{32}\text{Ar}$  populated in four- and six-nucleon removal reactions from  $^{36,38}\text{Ca}$  ions at intermediate energy were studied. From subsequent high-resolution  $\gamma$ -ray spectroscopy, a previously unknown 1900(4)-keV  $\gamma$  ray of  $^{32}\text{Ar}$  was identified. It is interpreted as the decay of a new excited state at 3767(5) keV into the  $2_1^+$  state. Shell-model calculations using the FSU cross-shell effective interaction suggest that it must be of mixed 0h-0p and 2p-2h nature to enable the observed  $\gamma$  decay to the  $sd$ -shell  $2_1^+$  state. From comparison to the mirror nucleus  $^{32}\text{Si}$ , two potential mirror states were identified; the  $2_2^+$  state, which requires the mixed character of the state in  $^{32}\text{Ar}$  to significantly alter its decay properties, a vanishing population cross section in  $2n$ -removal in contrast to theoretical predictions, and a large mirror-energy difference; or the  $0_2^+$  state, resulting in one of the largest MEDs ever reported. Calculations employing the SDPF-M shell-model effective interaction predict an intruder  $0^+$  state in the right energy range, potentially suggesting that its counterpart in the  $^{32}\text{Si}$  level scheme is hitherto unobserved. For  $\gamma$  decay to compete, it would, however, require a reduction of the spectroscopic factor for proton decay to the  $(1/2^+)$  state of  $^{31}\text{Cl}$  by a factor of roughly  $10^6$ . Indications of additional, unplaced  $\gamma$ -ray transitions of  $^{32}\text{Ar}$  at 2134(6) and 3161(7) keV were found but further experimental studies are needed to

corroborate their existence and also to confirm the placement of the 1900(4)-keV  $\gamma$  ray. Any chosen reaction mechanism has to facilitate a population of excited nuclear states with two protons in the  $pf$  shell. Inelastic proton scattering in inverse kinematics [65], for example, which has been shown to efficiently populate off-yrast states [66], might help to shed light on the nature of the 3767(5)-keV state. Conversely, the identification of a  $0^+$  state of  $^{32}\text{Si}$  at around 3.7 MeV, for instance in two-neutron transfer or  $\beta$ -decay experiments, has the potential to support a  $0^+$  assignment for the 3767(5)-keV state of  $^{32}\text{Ar}$ .

#### ACKNOWLEDGMENTS

The authors thank J. A. Tostevin for providing theoretical predictions of two-neutron removal cross sections. Discussions with W. Nazarewicz, A. Volya, and S. Wang are acknowledged. This work was supported by the U.S. NSF under Grants No. PHY-1565546 and No. PHY-2110365, by the DOE NNSA through the NSSC, under Award No. DE-NA0003180, and by the U.S. DOE, Office of Science, Office of Nuclear Physics, under Grants No. DE-SC0020451, No. DE-SC0023633 (MSU), and No. DE-FG02-87ER-40316 (WashU) and under Contract No. DE-AC02-06CH11357 (ANL). GRETINA was funded by the DOE, Office of Science. Operation of the array at NSCL was supported by the DOE under Grant No. DE-SC0019034.

---

[1] R. K. Wallace and S. E. Woosley, Explosive hydrogen burning, *Astrophys. J. Suppl. Series* **45**, 389 (1981).

[2] M. Pfützner, M. Karny, L. V. Grigorenko, and K. Riisager, Radioactive decays at limits of nuclear stability, *Rev. Mod. Phys.* **84**, 567 (2012).

[3] J. D. Holt, J. Menéndez, and A. Schwenk, Three-body forces and proton-rich nuclei, *Phys. Rev. Lett.* **110**, 022502 (2013).

[4] Y. Blumenfeld, T. Nilsson, and P. van Duppen, Facilities and methods for radioactive ion beam production, *Phys. Scr.* **2013**, 014023 (2013).

[5] M. Pfützner and C. Mazzocchi, Nuclei near and at the proton dripline, in *Handbook of Nuclear Physics*, edited by I. Tanihata, H. Toki, and T. Kajino (Springer Nature, Singapore, 2023), pp. 1295–1335.

[6] S. R. Stroberg, J. D. Holt, A. Schwenk, and J. Simonis, *Ab initio* limits of atomic nuclei, *Phys. Rev. Lett.* **126**, 022501 (2021).

[7] D. Kostyleva, I. Mukha, L. Acosta, E. Casarejos, V. Chudoba, A. A. Ciemny, W. Dominik, J. A. Dueñas, V. Dunin, J. M. Espino, A. Estradé, F. Farinon, A. Fomichev, H. Geissel, A. Gorshkov, L. V. Grigorenko, Z. Janas, G. Kamiński, O. Kiselev, R. Knöbel *et al.*, Towards the limits of existence of nuclear structure: Observation and first spectroscopy of the isotope  $^{31}\text{K}$  by measuring its three-proton decay, *Phys. Rev. Lett.* **123**, 092502 (2019).

[8] L. Lalanne, O. Sorlin, A. Poves, M. Assié, F. Hammache, S. Koyama, D. Suzuki, F. Flavigny, V. Girard-Alcindor, A. Lemasson, A. Matta, T. Roger, D. Beaumel, Y. Blumenfeld, B. A. Brown, F. De Oliveira Santos, F. Delaunay, N. de Séerville, S. Franchoo, J. Gibelin *et al.*,  $N = 16$  magicity revealed at the proton drip line through the study of  $^{35}\text{Ca}$ , *Phys. Rev. Lett.* **131**, 092501 (2023).

[9] I. Mukha, L. V. Grigorenko, X. Xu, L. Acosta, E. Casarejos, A. A. Ciemny, W. Dominik, J. Duéñas-Díaz, V. Dunin, J. M. Espino, A. Estradé, F. Farinon, A. Fomichev, H. Geissel, T. A. Golubkova, A. Gorshkov, Z. Janas, G. Kamiński, O. Kiselev, R. Knöbel *et al.*, Observation and spectroscopy of new proton-unbound isotopes  $^{30}\text{Ar}$  and  $^{29}\text{Cl}$ : An interplay of prompt two-proton and sequential decay, *Phys. Rev. Lett.* **115**, 202501 (2015).

[10] A. Gade, D. Bazin, B. A. Brown, C. M. Campbell, J. A. Church, D. C. Dinca, J. Enders, T. Glasmacher, P. G. Hansen, Z. Hu, K. W. Kemper, W. F. Mueller, H. Olliver, B. C. Perry, L. A. Riley, B. T. Roeder, B. M. Sherrill, J. R. Terry, J. A. Tostevin, and K. L. Yurkewicz, One-neutron knockout reactions on proton-rich nuclei with  $N = 16$ , *Phys. Rev. C* **69**, 034311 (2004).

[11] R. R. C. Clement, D. Bazin, W. Benenson, B. A. Brown, A. L. Cole, M. W. Cooper, P. A. DeYoung, A. Estrade, M. A. Famiano, N. H. Frank, A. Gade, T. Glasmacher, P. T. Hosmer, W. G. Lynch, F. Montes, W. F. Mueller, G. F. Peaslee, P. Santi, H. Schatz, B. M. Sherrill *et al.*, New approach for measuring properties of  $rp$ -process nuclei, *Phys. Rev. Lett.* **92**, 172502 (2004).

[12] A. R. L. Kennington, G. Lotay, D. T. Doherty, D. Seweryniak, C. Andreoiu, K. Auranen, M. P. Carpenter, W. N. Catford, C. M. Deibel, K. Hadyńska-Klęk, S. Hallam, D. E. M. Hoff, T. Huang, R. V. F. Janssens, S. Jazrawi, J. José, F. G. Kondev, T. Lauritsen, J. Li, A. M. Rogers *et al.*, Search for nova presolar grains:  $\gamma$ -

Ray spectroscopy of  $^{34}\text{Ar}$  and its relevance for the astrophysical  $^{33}\text{Cl}(p, \gamma)$  reaction, *Phys. Rev. Lett.* **124**, 252702 (2020).

[13] K. Blaum, G. Audi, D. Beck, G. Bollen, F. Herfurth, A. Kellerbauer, H.-J. Kluge, E. Sauvan, and S. Schwarz, Masses of  $^{32}\text{Ar}$  and  $^{33}\text{Ar}$  for fundamental tests, *Phys. Rev. Lett.* **91**, 260801 (2003).

[14] B. Blank, N. Adimi, M. Alcorta, A. Bey, M. J. G. Borge, B. A. Brown, F. de Oliveira Santos, C. Dossat, H. O. U. Fynbo, J. Giovinazzo, H. H. Knudsen, M. Madurga, A. Magilligan, I. Matea, A. Perea, K. Sümmerer, O. Tengblad, and J. C. Thomas, Detailed study of the decay of  $^{32}\text{Ar}$ , *Eur. Phys. J. A* **57**, 28 (2021).

[15] A. Gade, D. Bazin, B. A. Brown, C. M. Campbell, J. A. Church, D. C. Dinca, J. Enders, T. Glasmacher, P. G. Hansen, Z. Hu, K. W. Kemper, W. F. Mueller, H. Olliver, B. C. Perry, L. A. Riley, B. T. Roeder, B. M. Sherrill, J. R. Terry, J. A. Tostevin, and K. L. Yurkewicz, Reduced occupancy of the deeply bound  $0d_{5/2}$  neutron state in  $^{32}\text{Ar}$ , *Phys. Rev. Lett.* **93**, 042501 (2004).

[16] A. Gade, P. Adrich, D. Bazin, M. D. Bowen, B. A. Brown, C. M. Campbell, J. M. Cook, T. Glasmacher, P. G. Hansen, K. Hosier, S. McDaniel, D. McGlinchery, A. Obertelli, K. Siwek, L. A. Riley, J. A. Tostevin, and D. Weisshaar, Reduction of spectroscopic strength: Weakly-bound and strongly-bound single-particle states studied using one-nucleon knockout reactions, *Phys. Rev. C* **77**, 044306 (2008).

[17] J. A. Tostevin and A. Gade, Systematics of intermediate-energy single-nucleon removal cross sections, *Phys. Rev. C* **90**, 057602 (2014).

[18] J. A. Tostevin and A. Gade, Updated systematics of intermediate-energy single-nucleon removal cross sections, *Phys. Rev. C* **103**, 054610 (2021).

[19] C. Ouellet and B. Singh, Nuclear data sheets for  $a = 32$ , *Nucl. Data Sheets* **112**, 2199 (2011).

[20] P. D. Cottle, Z. Hu, B. V. Pritychenko, J. A. Church, M. Fauerbach, T. Glasmacher, R. W. Ibbotson, K. W. Kemper, L. A. Riley, H. Scheit, and M. Steiner,  $0^+_{\text{gs}} \rightarrow 2^+_1$  excitations in the mirror nuclei  $^{32}\text{Ar}$  and  $^{32}\text{Si}$ , *Phys. Rev. Lett.* **88**, 172502 (2002).

[21] A. Bürger, F. Azaiez, M. Stanoi, Z. Dombrádi, A. Algora, A. Al-Khatib, B. Bastin, G. Benzoni, R. Borcea, C. Bourgeois, P. Bringel, E. Clément, J.-C. Dalouzy, Z. Dlouhý, A. Drouart, C. Engelhardt, S. Franchoo, Z. Fülop, A. Görzen, S. Grévy *et al.*, Spectroscopy around  $^{36}\text{Ca}$ , *Acta Phys. Pol. B* **38**, 1353 (2007).

[22] K. Yoneda, A. Obertelli, A. Gade, D. Bazin, B. A. Brown, C. M. Campbell, J. M. Cook, P. D. Cottle, A. D. Davies, D.-C. Dinca, T. Glasmacher, P. G. Hansen, T. Hoagland, K. W. Kemper, J.-L. Lecouey, W. F. Mueller, R. R. Reynolds, B. T. Roeder, J. R. Terry, J. A. Tostevin *et al.*, Two-neutron knockout from neutron-deficient  $^{34}\text{Ar}$ ,  $^{30}\text{S}$ , and  $^{26}\text{Si}$ , *Phys. Rev. C* **74**, 021303(R) (2006).

[23] M. Wang, W. J. Huang, F. G. Kondev, G. Audi, and S. Naimi, The AME 2020 atomic mass evaluation (II). Tables, graphs and references, *Chin. Phys. C* **45**, 030003 (2021).

[24] N. Dronchi, D. Weisshaar, B. A. Brown, A. Gade, R. J. Charity, L. G. Sobotka, K. W. Brown, W. Reviol, D. Bazin, P. J. Farris, A. M. Hill, J. Li, B. Longfellow, D. Rhodes, S. N. Paneru, S. A. Gillespie, A. Anthony, E. Rubino, and S. Biswas, Measurement of the  $B(E2 \uparrow)$  strengths of  $^{36}\text{Ca}$  and  $^{38}\text{Ca}$ , *Phys. Rev. C* **107**, 034306 (2023).

[25] A. Gade, D. Weisshaar, B. A. Brown, J. A. Tostevin, D. Bazin, K. Brown, R. J. Charity, P. J. Farris, A. M. Hill, J. Li, B. Longfellow, W. Reviol, and D. Rhodes, In-beam  $\gamma$ -ray spectroscopy at the proton dripline:  $^{40}\text{Sc}$ , *Phys. Lett. B* **808**, 135637 (2020).

[26] A. Gade, D. Weisshaar, B. A. Brown, D. Bazin, K. W. Brown, R. J. Charity, P. Farris, A. M. Hill, J. Li, B. Longfellow, D. Rhodes, W. Reviol, and J. A. Tostevin, Exploiting dissipative reactions to perform in-beam  $\gamma$ -ray spectroscopy of the neutron-deficient isotopes  $^{38,39}\text{Ca}$ , *Phys. Rev. C* **106**, 064303 (2022).

[27] A. Gade, B. A. Brown, D. Weisshaar, D. Bazin, K. W. Brown, R. J. Charity, P. Farris, A. M. Hill, J. Li, B. Longfellow, D. Rhodes, W. Reviol, and J. A. Tostevin, Dissipative reactions with intermediate-energy beams: A novel approach to populate complex-structure states in rare isotopes, *Phys. Rev. Lett.* **129**, 242501 (2022).

[28] T. Beck, A. Gade, B. A. Brown, J. A. Tostevin, D. Weisshaar, D. Bazin, K. W. Brown, R. J. Charity, P. J. Farris, S. A. Gillespie, A. M. Hill, J. Li, B. Longfellow, W. Reviol, and D. Rhodes, Probing proton cross-shell excitations through the two-neutron removal from  $^{38}\text{Ca}$ , *Phys. Rev. C* **108**, L061301 (2023).

[29] T. Beck, A. Gade, B. A. Brown, D. Weisshaar, D. Bazin, K. W. Brown, R. J. Charity, P. J. Farris, S. A. Gillespie, A. M. Hill, J. Li, B. Longfellow, W. Reviol, and D. Rhodes, In-beam  $\gamma$ -ray spectroscopy of negative-parity states of  $^{37}\text{K}$  populated in dissipative reactions, *Phys. Rev. C* **110**, 014305 (2024).

[30] A. Gade and B. M. Sherrill, NSCL and FRIB at Michigan State University: Nuclear science at the limits of stability, *Phys. Scr.* **91**, 053003 (2016).

[31] D. J. Morrissey, B. M. Sherrill, M. Steiner, A. Stolz, and I. Wiedenhoever, Commissioning the A1900 projectile fragment separator, *Nucl. Instrum. Methods Phys. Res., Sect. B* **204**, 90 (2003).

[32] D. Bazin, J. Caggiano, B. Sherrill, J. Yurkon, and A. Zeller, The S800 spectrograph, *Nucl. Instrum. Methods Phys. Res., Sect. B* **204**, 629 (2003).

[33] J. Yurkon, D. Bazin, W. Benenson, D. J. Morrissey, B. M. Sherrill, D. Swan, and R. Swanson, Focal plane detector for the S800 high-resolution spectrometer, *Nucl. Instrum. Methods Phys. Res., Sect. A* **422**, 291 (1999).

[34] S. Paschalidis, I. Y. Lee, A. O. Macchiavelli, C. M. Campbell, M. Cromaz, S. Gros, J. Pavan, J. Qian, R. M. Clark, H. L. Crawford, D. Doering, P. Fallon, C. Lionberger, T. Loew, M. Petri, T. Stezelberger, S. Zimmermann, D. C. Radford, K. Lagergren, D. Weisshaar *et al.*, The performance of the Gamma-ray energy tracking in-beam nuclear array GRETINA, *Nucl. Instrum. Methods Phys. Res., Sect. A* **709**, 44 (2013).

[35] D. Weisshaar, D. Bazin, P. C. Bender, C. M. Campbell, F. Recchia, V. Bader, T. Baugher, J. Belarge, M. P. Carpenter, H. L. Crawford, M. Cromaz, B. Elman, P. Fallon, A. Forney, A. Gade, J. Harker, N. Kobayashi, C. Langer, T. Lauritsen, I. Y. Lee *et al.*, The performance of the  $\gamma$ -ray tracking array GRETINA for  $\gamma$ -ray spectroscopy with fast beams of rare isotopes, *Nucl. Instrum. Methods Phys. Res., Sect. A* **847**, 187 (2017).

[36] A. Obertelli, A. Gade, D. Bazin, C. M. Campbell, J. M. Cook, P. D. Cottle, A. D. Davies, D.-C. Dinca, T. Glasmacher, P. G. Hansen, T. Hoagland, K. W. Kemper, J.-L. Lecouey, W. F. Mueller, R. R. Reynolds, B. T. Roeder, J. R. Terry, J. A. Tostevin, K. Yoneda, and H. Zwahlen, Population of bound excited states in intermediate-energy fragmentation reactions, *Phys. Rev. C* **73**, 044605 (2006).

[37] B. Longfellow, A. Gade, D. Bazin, P. C. Bender, M. Bowry, B. A. Brown, B. Elman, E. Lunderberg, D. Rhodes, M. Spieker, D. Weisshaar, and S. J. Williams, Relative population of states in  $^{21}\text{Mg}$  from few-nucleon removal reactions, *Phys. Rev. C* **107**, 014620 (2023).

[38] J. Henderson and S. R. Stroberg, Examination of the inversion of isobaric analogue states in mirror nuclei, *Phys. Rev. C* **102**, 031303(R) (2020).

[39] L. Lalanne, O. Sorlin, A. Poves, M. Assié, F. Hammache, S. Koyama, D. Suzuki, F. Flavigny, V. Girard-Alcindor, A. Lemasson, A. Matta, T. Roger, D. Beaumel, Y. Blumenfeld, B. A. Brown, F. De Oliveira Santos, F. Delaunay, N. de Séreville, S. Franchoo, J. Gibelin *et al.*, Structure of  $^{36}\text{Ca}$  under the coulomb magnifying glass, *Phys. Rev. Lett.* **129**, 122501 (2022).

[40] B. A. Brown and W. D. M. Rae, The Shell-Model Code NuShellX@MSU, *Nucl. Data Sheets* **120**, 115 (2014).

[41] R. S. Lubna, K. Kravvaris, S. L. Tabor, V. Tripathi, A. Volya, E. Rubino, J. M. Allmond, B. Abromeit, L. T. Baby, and T. C. Hensley, Structure of  $^{38}\text{Cl}$  and the quest for a comprehensive shell model interaction, *Phys. Rev. C* **100**, 034308 (2019).

[42] R. S. Lubna, K. Kravvaris, S. L. Tabor, V. Tripathi, E. Rubino, and A. Volya, Evolution of the  $N = 20$  and 28 shell gaps and two-particle-two-hole states in the FSU interaction, *Phys. Rev. Res.* **2**, 043342 (2020).

[43] L. V. Grigorenko, I. G. Mukha, and M. V. Zhukov, Prospective candidates for the two-proton decay studies. (II) Exploratory studies of  $^{30}\text{Ar}$ ,  $^{34}\text{Ca}$ , and  $^{45}\text{Fe}$ , *Nucl. Phys. A* **714**, 425 (2003).

[44] Y. Utsuno, T. Otsuka, T. Mizusaki, and M. Honma, Varying shell gap and deformation in  $N \sim 20$  unstable nuclei studied by the Monte Carlo shell model, *Phys. Rev. C* **60**, 054315 (1999).

[45] Y. Utsuno, T. Otsuka, T. Mizusaki, and M. Honma, Extreme location of F drip line and disappearance of the  $N = 20$  magic structure, *Phys. Rev. C* **64**, 011301(R) (2001).

[46] N. Shimizu, T. Mizusaki, Y. Utsuno, and Y. Tsunoda, Thick-restart block Lanczos method for large-scale shell-model calculations, *Comput. Phys. Commun.* **244**, 372 (2019).

[47] F. Rotaru, F. Negoita, S. Grévy, J. Mrazek, S. Lukyanov, F. Nowacki, A. Poves, O. Sorlin, C. Borcea, R. Borcea, A. Buta, L. Cáceres, S. Calinescu, R. Chevrier, Z. Dombrádi, J. M. Daugas, D. Lebhardt, Y. Penionzhkevich, C. Petrone, D. Sohler *et al.*, Unveiling the intruder deformed  $0_2^+$  state in  $^{34}\text{Si}$ , *Phys. Rev. Lett.* **109**, 092503 (2012).

[48] B. A. Brown, The nuclear shell model towards the drip lines, *Physics* **4**, 525 (2022).

[49] J. G. Pronko and R. E. McDonald, Study of  $^{32}\text{Si}$  using the  $^{30}\text{Si}(t, p\gamma)$  reaction, *Phys. Rev. C* **6**, 2065 (1972).

[50] W. Chung, Empirical renormalization of shell-model Hamiltonians and magnetic dipole moments of sd-shell nuclei, Ph.D. thesis, Michigan State University, 1977, [https://publications.nscl.msu.edu/thesis/Chung\\_1976\\_31.pdf](https://publications.nscl.msu.edu/thesis/Chung_1976_31.pdf).

[51] H. T. Fortune, L. Bland, D. L. Watson, and M. A. Abouzeid,  $^{32}\text{Si}$  from  $^{30}\text{Si}(t, p)$ , *Phys. Rev. C* **25**, 5 (1982).

[52] J. B. Ehrman, On the displacement of corresponding energy levels of  $\text{C}^{13}$  and  $\text{N}^{13}$ , *Phys. Rev.* **81**, 412 (1951).

[53] R. G. Thomas, An analysis of the energy levels of the mirror nuclei,  $\text{C}^{13}$  and  $\text{N}^{13}$ , *Phys. Rev.* **88**, 1109 (1952).

[54] I. Stefan, F. de Oliveira Santos, O. Sorlin, T. Davinson, M. Lewitowicz, G. Dumitru, J. C. Angélique, M. Angélique, E. Berthoumieux, C. Borcea, R. Borcea, A. Buta, J. M. Daugas, F. de Grancey, M. Fadil, S. Grévy, J. Kiener, A. Lefebvre-Schuhl, M. Lenhardt, J. Mrazek *et al.*, Probing nuclear forces beyond the drip-line using the mirror nuclei  $^{16}\text{N}$  and  $^{16}\text{F}$ , *Phys. Rev. C* **90**, 014307 (2014).

[55] B. Longfellow, A. Gade, J. A. Tostevin, E. C. Simpson, B. A. Brown, A. Magilligan, D. Bazin, P. C. Bender, M. Bowry, B. Elman, E. Lunderberg, D. Rhodes, M. Spieker, D. Weisshaar, and S. J. Williams, Two-neutron knockout as a probe of the composition of states in  $^{22}\text{Mg}$ ,  $^{23}\text{Al}$ , and  $^{24}\text{Si}$ , *Phys. Rev. C* **101**, 031303(R) (2020).

[56] R. J. Charity, K. W. Brown, J. Okołowicz, M. Płoszajczak, J. M. Elson, W. Reviol, L. G. Sobotka, W. W. Buhro, Z. Chajecki, W. G. Lynch, J. Manfredi, R. Shane, R. H. Showalter, M. B. Tsang, D. Weisshaar, J. R. Winkelbauer, S. Bedoor, and A. H. Wuosmaa, Invariant-mass spectroscopy of  $^{14}\text{O}$  excited states, *Phys. Rev. C* **100**, 064305 (2019).

[57] M. Shamsuzzoha Basunia and A. Chakraborty, Nuclear data sheets for  $A = 30$ , *Nucl. Data Sheets* **197**, 1 (2024).

[58] N. Nica and B. Singh, Nuclear data sheets for  $A = 34$ , *Nucl. Data Sheets* **113**, 1563 (2012).

[59] A. Zilges, P. von Brentano, A. Richter, R. D. Heil, U. Kneissl, H. H. Pitz, and C. Wesselborg, Uncommon decay branching ratios of spin-one states in the rare-earth region and evidence for  $K$  mixing, *Phys. Rev. C* **42**, 1945 (1990).

[60] T. Beck, V. Werner, N. Pietralla, M. Bhike, N. Cooper, U. Friman-Gayer, J. Isaak, R. V. Jolos, J. Kleemann, Krishchayan, O. Papst, W. Tornow, C. Bernards, B. P. Crider, R. S. Iliev, B. Löher, C. Mihai, F. Naqvi, S. Pascu, E. E. Peters *et al.*,  $\Delta K = 0 M1$  excitation strength of the well-deformed nucleus  $^{164}\text{Dy}$  from  $K$  mixing, *Phys. Rev. Lett.* **125**, 092501 (2020).

[61] N. Dronchi, R. J. Charity, L. G. Sobotka, B. A. Brown, D. Weisshaar, A. Gade, K. W. Brown, W. Reviol, D. Bazin, P. J. Farris, A. M. Hill, J. Li, B. Longfellow, D. Rhodes, S. N. Paneru, S. A. Gillespie, A. K. Anthony, E. Rubino, and S. Biswas, Evolution of shell gaps in the neutron-poor calcium region from invariant-mass spectroscopy of  $^{37,38}\text{Sc}$ ,  $^{35}\text{Ca}$ , and  $^{34}\text{K}$ , *Phys. Rev. C* **110**, L031302 (2024).

[62] E. Caurier, K. Langanke, G. Martínez-Pinedo, F. Nowacki, and P. Vogel, Shell model description of isotope shifts in calcium, *Phys. Lett. B* **522**, 240 (2001).

[63] J. A. Tostevin, G. Podolyák, B. A. Brown, and P. G. Hansen, Correlated two-nucleon stripping reactions, *Phys. Rev. C* **70**, 064602 (2004).

[64] J. A. Tostevin and B. A. Brown, Diffraction dissociation contributions to two-nucleon knockout reactions and the suppression of shell-model strength, *Phys. Rev. C* **74**, 064604 (2006).

[65] A. Gade and T. Glasmacher, In-beam nuclear spectroscopy of bound states with fast exotic ion beams, *Prog. Part. Nucl. Phys.* **60**, 161 (2008).

[66] L. A. Riley, D. Bazin, J. Belarge, P. C. Bender, B. A. Brown, P. D. Cottle, B. Elman, A. Gade, S. D. Gregory, E. B. Haldeman, K. W. Kemper, B. R. Klybor, M. A. Liggett, S. Lipschutz, B. Longfellow, E. Lunderberg, T. Mijatovic, J. Pereira, L. M. Skiles, R. Titus *et al.*, Inverse-kinematics proton scattering from  $^{42,44}\text{S}$ ,  $^{41,43}\text{P}$ , and the collapse of the  $N = 28$  major shell closure, *Phys. Rev. C* **100**, 044312 (2019).